

Some Ligands Enhance the Efflux of Other Ligands by the *Escherichia coli* Multidrug Pump AcrB

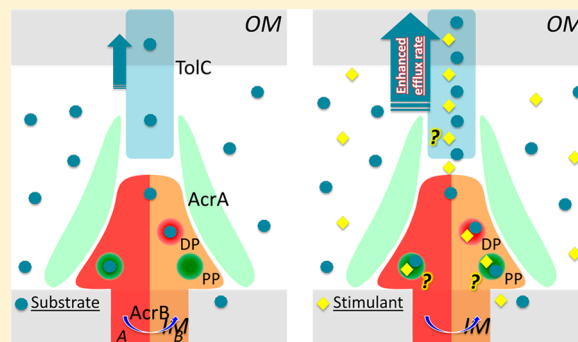
Alfred D. Kinana,[†] Attilio V. Vargiu,[‡] and Hiroshi Nikaido^{*,†}

[†]Department of Molecular and Cell Biology, University of California, Berkeley California 94720, United States

[‡]Department of Physics, University of Cagliari, S.P. 8 km 0.700, Monserrato (CA) 09042, Italy

S Supporting Information

ABSTRACT: By measuring quantitatively the active efflux of cephalosporins by the RND (resistance-nodulation-division) family efflux pump AcrB in intact cells of *Escherichia coli*, we found that the simultaneous presence of another substrate, such as chloramphenicol, benzene, cyclohexane, or Arg β -naphthylamide, significantly enhanced the extrusion of cephalosporins. The stimulation occurred also in a strain expressing the covalently linked trimer of AcrB, and thus cannot be ascribed to the enhanced assembly of the trimer from AcrB monomers. When Val139 of AcrB was changed into Phe, the stimulation by benzene was found to occur at much lower concentration of the solvent. A plausible explanation of these observations is that the AcrB pump is constructed to pump out very rapidly the solvent or chloramphenicol molecules, and thus the efflux of cephalosporins, which presumably bind to a different subsite within the large binding pocket of AcrB, can become facilitated. Computer simulations of ligand binding to AcrB, both by docking and by molecular dynamics simulations, produced results supporting and extending this hypothesis. Benzene and the cephalosporin nitrocefin can bind simultaneously to the distal binding pocket of AcrB, both in the wild type and in the V139F variant. Interestingly, while the binding position and strength of benzene are almost unaffected by the presence of nitrocefin, this latter substrate is significantly displaced toward the exit gate in both wild type and mutant transporter in the presence of benzene. Additionally, the cephalosporin efflux may be enhanced by the binding of solvents (sometimes to the cephalosporin-free protomer), which could accelerate AcrB conformational changes necessary for substrate extrusion.



The RND (resistance-nodulation-division) family of transporters,¹ such as AcrB of *Escherichia coli*, pump out drug molecules mostly from the periplasm of Gram-negative bacteria directly into the external medium, through collaboration with an outer membrane channel (TolC in the case of AcrB) and a periplasmic accessory protein (AcrA in the case of AcrB).² Some of these transporters, including AcrB, handle a very wide range of ligands, including antibiotics, biocides, dyes, detergents,³ and even simple solvents.^{4,5} In our previous attempt to predict the binding of these ligands to the deep binding pocket of the AcrB protein,⁶ we used the computer prediction algorithm of Autodock Vina and found that some ligands, including nitrocefin, bind to the narrow “groove” of the pocket, whereas others, including chloramphenicol and benzene, bound to a much wider “cave” area of this large pocket. We examined whether the simultaneous presence of two ligands results in competition. As we can measure the efflux of nitrocefin in a quantitative, real-time assay,⁷ this was followed in the presence of minocycline, a groove-binder, and of chloramphenicol, a cave-binder. The results showed that minocycline strongly inhibited the efflux of nitrocefin presumably by interfering with the binding of the latter to

the groove, whereas there was no evidence of inhibition when chloramphenicol was added.⁶

Examination of chloramphenicol data suggested in addition that the drug, especially at higher concentrations, actually may enhance, rather than inhibit, the efflux of nitrocefin. Because such mutual stimulation between ligands, if true, may shed light into the mechanism of efflux transport, we began by confirming the reproducibility of these data. We then found that other ligands, especially solvents such as benzene and cyclohexane, which are substrates of the AcrB pump,^{4,5} strongly accelerated the efflux of nitrocefin and another cephalosporin, cefamandole. We examined the binding of both nitrocefin and benzene to AcrB both by computer docking and by molecular dynamics simulation and discuss possible mechanisms of this stimulation phenomenon.

EXPERIMENTAL PROCEDURES

Bacterial Strains. For the measurement of cephalosporin efflux, *E. coli* K12 strains HN1157 and HN1160⁷ were used for

Received: September 19, 2013

Revised: October 23, 2013

Published: October 25, 2013



nitrocefin and cefamandole, respectively. In both of these strains, the expression of the AcrAB efflux pump was increased by the deletion of the *acrR* repressor gene. HN1157 also contained a mutated porin gene producing a larger pore channel, so that the influx of nitrocefin across the outer membrane was facilitated. In HN1160, the endogenous AmpC β -lactamase, with low K_M values for cephalosporins, was replaced by the TEM β -lactamase with much higher K_M values.

Culture of Strains and Nitrocefin Efflux Assay in the Presence and Absence of Other Substrates. Strains were grown in M63 medium ((NH_4)₂SO₄ 15 mM; MgSO₄ 1 mM; FeSO₄ 1.3 μ M; 0.1 M K-phosphate buffer at pH 7.0; 0.2% glucose) at 30 °C with shaking until the cell culture reached an OD₆₀₀ of 0.65. For the growth of HN1160, arginine (20 μ g/mL) and thiamine (1 μ g/mL) were added to this medium. Cells were harvested by centrifugation, washed twice, and resuspended in 50 mM potassium phosphate buffer, pH 7.0 containing 5 mM MgCl₂ to a final OD₆₀₀ of 0.8. Samples were split into two sets of cuvettes. In one set, a stimulator substrate was added to a specified final concentration. In the other set, no substrate was added. Samples were preincubated at room temperature for 5–10 min. Nitrocefin or cefamandole was then added, and efflux assays were performed as described previously.⁷

Construction of an *acrB* Mutant and Gene Replacement in *E. coli* Genome. First, the wild type sequence of *acrB* from HN1157⁷ was amplified by PCR and cloned into pSPORT1 vector between BamHI and SmaI restriction sites. The mutation V139F was introduced by site-directed mutagenesis using QuickChange II Site-Directed Mutagenesis Kit (Agilent) as directed by the manufacturer. The mutant gene was then subcloned into pKO3 vector⁸ between BamHI and SmaI restriction sites, giving pKO3/*acrB*_V139F plasmid. This plasmid was electroporated into HN1157, the chromosomal integrates were selected at 42°C, and the strains that lost the vector sequence was selected with 5% sucrose,⁸ resulting in the strains in which the *acrB* gene was replaced with the mutant gene coding for the V139F sequence. Gene replacement was confirmed by PCR using a forward primer annealing on *acrA* and a reverse primer annealing on *acrB*, followed by DNA sequencing. The oligonucleotide primers used for PCR amplification and site-directed mutagenesis are shown in Table 1 of the Supporting Information.

Determination of Minimal Inhibitory Concentration (MIC). MIC of nitrocefin was determined in the presence and absence of 32 μ g/mL Arg β -naphthylamine, by streaking a culture of HN1157 on an LB plate containing a linear gradient of nitrocefin (0–25 μ g/mL) and by incubating the plate overnight at 37 °C.

Docking and MD simulations. In the bimolecular complexes the starting position of each substrate within the distal pocket of the binding protomer (for MD simulation) was taken either from our previous study⁹ or from docking calculations performed with the AUTODOCK VINA package¹⁰ using as a target the crystal structure of AcrB¹¹ (wt protein) and that resulting from structural relaxation of mutant AcrB free of substrates (V139F variant). The latter model was constructed by introducing the V139F mutation in the binding protomer of the AcrB model 2J8S¹¹ through the mutator plugin of VMD,¹² following the procedure described earlier.¹³ After preliminary energy minimization by this program, the structure was optimized by MD simulation.

In the trimolecular complexes, the second ligand was docked on the two top conformations extracted from the MD simulation of bimolecular complexes, by a cluster analysis performed on the equilibrium trajectories. Further details are described in Supporting Information.

The setup for the MD simulations of bi- and trimolecular complexes was identical to that reported previously.⁹ A reduced model of the protein was used, only including the periplasmic loops responsible for the substrate specificity of AcrB.¹⁴ Further details and calculation of binding energy through MM/GBSA approach and metadynamics are described in Supporting Information.

RESULTS

Nitrocefin Efflux Is Stimulated by Chloramphenicol. In our previous study comparing the effects of minocycline and chloramphenicol on the efflux of nitrocefin,⁶ we noted that the former acted as a powerful inhibitor, whereas the latter showed no visible inhibition. A careful examination of these data showed that there was a slight stimulation of nitrocefin efflux in the presence of chloramphenicol; however, at that time only efflux rates at different external concentrations of nitrocefin were compared. To confirm that the stimulation was real, a more thorough analysis was performed in which we examined the precise kinetics of efflux, by plotting the efflux rates at different nitrocefin concentrations in the periplasm, where its capture takes place.⁷ Such an analysis (Figure 1) showed that the stimulation was slight but real, mainly resulting from approximately 20% increase in V_{max} and possibly also from a decrease in K_M (less than 10%).

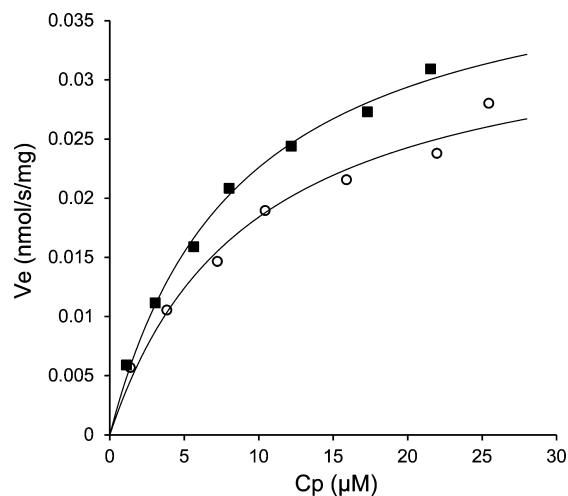


Figure 1. Chloramphenicol stimulates the efflux of nitrocefin. The efflux rate (V_e) of nitrocefin is plotted against its periplasmic concentration (C_p). Measurement was carried out in the absence (○) and presence (■) of 0.1 mM chloramphenicol. This experiment was repeated and gave essentially identical results.

Nitrocefin Efflux Is Stimulated by Solvents. We tried to find other AcrB substrates that stimulated the efflux of nitrocefin more strongly, so that further analysis would become facilitated. High concentrations (30 mM) of both benzene and cyclohexane produced strong stimulation of nitrocefin efflux (Figure 2A and B). Similarly, 25 mM cyclohexanone produced a remarkable activation of nitrocefin flux (Figure 2C). We examined the possibility that the solvents might be directly interfering with the hydrolysis of nitrocefin catalyzed by the

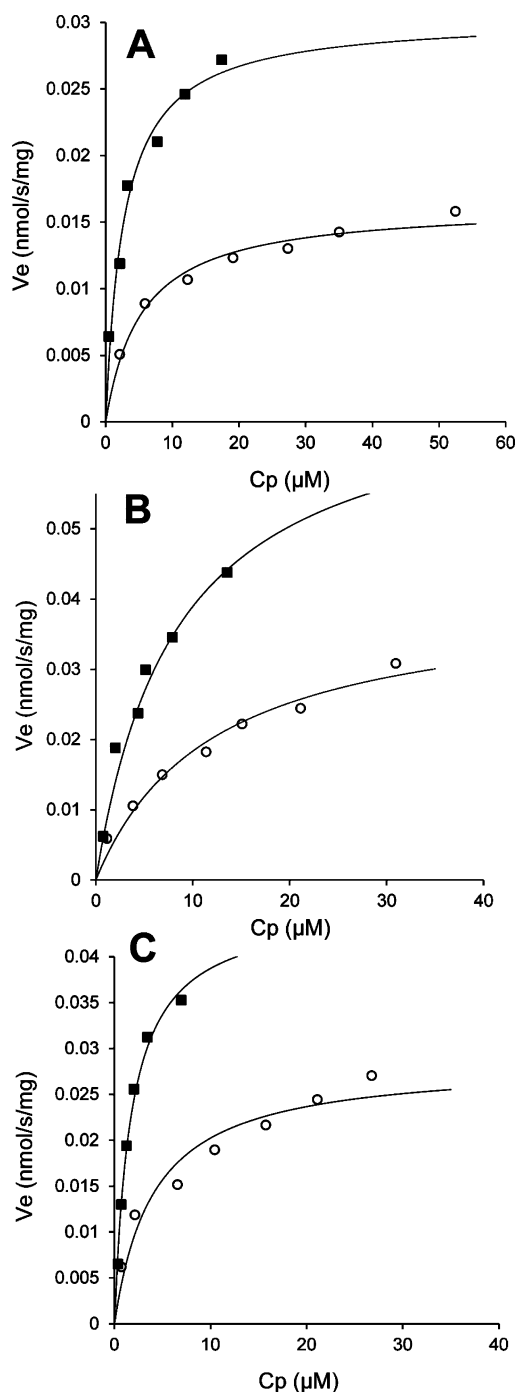


Figure 2. Stimulation of nitrocefin efflux by high concentrations (30 mM) of benzene (A) and cyclohexane (B) and 25 mM cyclohexanone (C). Benzene and cyclohexane were added as a 1:1 (v:v) mixture with ethanol, and the same volume of 50% aqueous ethanol was added to the control. Cyclohexanone was similarly added as a 1:1 mixture with dimethylsulfoxide. As in Figure 1, the efflux rates of nitrocefin (V_e) are plotted against its periplasmic concentrations (C_p). Measurement was carried out in the absence (○) and presence (■) of solvents. These experiments were repeated several times for each solvent, and reproducible results were obtained.

AmpC β -lactamase. However, the solvents had no effect on nitrocefin hydrolysis by the sonicated cell extracts. At these high concentrations, solvents caused increases in the V_{\max} values and often decreased the values of K_M ; for example, in two

experiments with benzene, V_{\max} was increased about 2-fold, and K_M was also decreased 2-fold (not shown).

Although these results were encouraging, solvents were used at concentrations much higher than that of the measured efflux substrate, nitrocefin. At such concentrations we cannot exclude the possibility that solvent effect was caused by their strong partition into the bilayer, which may affect the function of the transporter. (However, this mechanism is unlikely in the V139F mutant AcrB described below.) At concentrations comparable to the nitrocefin concentration, i.e., around 0.1 mM, the effect was more modest, although a clear indication of stimulation was seen (see below). We have tested a number of other potential substrates of the AcrB pump at 0.1 mM concentration. We could not find any evidence of stimulation of nitrocefin efflux in the presence of the following substrates: deoxycholate, taurocholate, novobiocin, erythromycin, azithromycin, and nalidixic acid (results not shown).

Nitrocefin Efflux Is Stimulated by Arg β -Naphthylamide. The well-known AcrB inhibitor (and substrate¹⁵) Phe-Arg β -naphthylamide inhibited nitrocefin efflux when used at a low concentration (20 μ M), but at a higher concentration (0.1 mM) it often produced stimulation (results not shown). Although this compound was recently reported to increase the nonspecific permeability of the outer membrane,^{16,17} such an effect at high concentrations was known already at the time of its discovery,¹⁵ and its activity as an efflux inhibitor is supported by a large number of studies.¹⁸ Because Phe-Arg β -naphthylamide is hydrolyzed by intact *E. coli* cells first into Phe and Arg β -naphthylamide by peptidase N (T. May and H. Nikaido, unpublished), Arg β -naphthylamide was tested and indeed found to be a powerful stimulant of nitrocefin efflux (Figure 3). A large decrease in the values of K_M ($81 \pm 6.3\%$

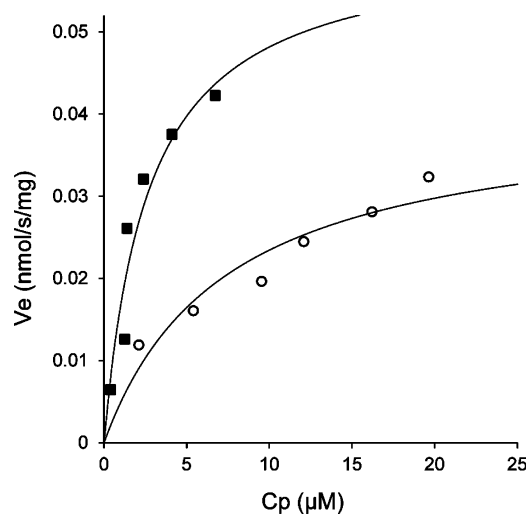


Figure 3. Stimulation of nitrocefin efflux by 0.1 mM Arg- β -naphthylamide. As in Figure 1, V_e of nitrocefin is plotted against its C_p . Measurement was carried out in the absence (○) and presence (■) of Arg- β -naphthylamide. This experiment was repeated several times, and reproducible data were obtained (see text).

decrease in four experiments) played a major part here, although there was also a modest increase in V_{\max} in all experiments. Neither Phe nor the further hydrolysis product of Arg β -naphthylamide, Arg and β -naphthylamine, produced significant stimulation (or inhibition).

When nitrocefin MIC was determined by using the gradient plate method in the presence of 32 $\mu\text{g/mL}$ (0.107 mM) Arg β -naphthylamide, there was a slight but reproducible increase in MIC, from 11.1 to 13.1 $\mu\text{g/mL}$, consistent with the stimulation of nitrocefin efflux (Supplementary Figure S1). Although the increase was smaller than expected, this could be due to the instability of the stimulator, Arg β -naphthylamide, which is hydrolyzed by peptidase N.

Efflux of Cefamandole Is Also Stimulated by Solvents and Chloramphenicol. Nitrocefin binds very tightly to the distal binding pocket of AcrB,⁹ and its transport K_M is by far the lowest among the cephalosporins tested.⁷ In order to show that the stimulation phenomenon is not solely limited to this tight-binding substrate, we used cefamandole, which is expected to bind less tightly than nitrocefin to the binding site, with the calculated binding energy (in docking with Autodock Vina) of -9.2 kcal/mol in contrast to that of -10.2 kcal/mol for nitrocefin. Indeed, cefamandole is pumped out by AcrB with a much higher $K_{0.5}$ value of around 20 μM compared with the K_M of nitrocefin (around 5 μM).⁷ Cefamandole efflux was indeed stimulated by 0.1 mM and 30 mM benzene (Figure 4A and B) reproducibly. Chloramphenicol (0.1 mM) also produced a significant stimulation of cefamandole efflux (Figure 4C). The efflux kinetics of cefamandole shows a strong cooperativity,⁷ and thus its analysis becomes more complicated. However, the stimulation again seems to be caused mainly by increases in V_{\max} and decreases in $K_{0.5}$. Interestingly, in all experiments there appeared to be a significant decrease in apparent cooperativity, the calculated Hill coefficients decreasing to 63%, 81%, 81%, and 91% of the no-solvent control value (average 2.69) in the four experiments with 30 mM benzene.

Stimulation of Nitrocefin Efflux Is Not Caused by the Accelerated Assembly of AcrB Trimer. According to the functionally rotating trimer concept of AcrB function, AcrB cannot perform its efflux function unless it is assembled into a homotrimer. Thus it is possible that solvents stimulate the efflux by somehow facilitating the assembly of the AcrB trimer. This was tested by using the covalently linked, giant AcrB trimer produced from the modified gene coding for such a complex.¹⁹ The stimulatory effect of benzene was indeed confirmed in the linked trimer (Figure 5).

Studies with the V139F Mutant AcrB. The results presented above suggested that the effect of stimulants (such as solvents) is likely to involve the interaction (either direct or allosteric) of these ligands and cephalosporins in an AcrB trimer. In an effort to understand how this interaction could occur within the large (distal) binding pocket of AcrB, docking prediction was made with Autodock Vina. The calculated binding energy of benzene to the AcrB binding pocket was quite small (-5.1 kcal/mol), and it appeared to bind to the lower (i.e., closer to the membrane surface) part of the binding pocket, earlier called “cave”,⁶ at a location closest to the Val139 residue (with the closest distance of 3.2 Å) (Figure 6). We thus tried to strengthen the binding of benzene to this region of the binding pocket by mutating Val139 to a Phe residue. This mutation was constructed, and the wild type *acrB* gene was replaced by this mutant gene as described in Experimental Procedures.

When nitrocefin efflux was measured in this mutant, a much stronger stimulation by 0.1 mM benzene was observed (Figure 7B), in comparison with the cells producing the wild type AcrB (Figure 7A). In the mutant, stimulation was apparently caused by an increase (about 60%) in V_{\max} and a strong decrease (by

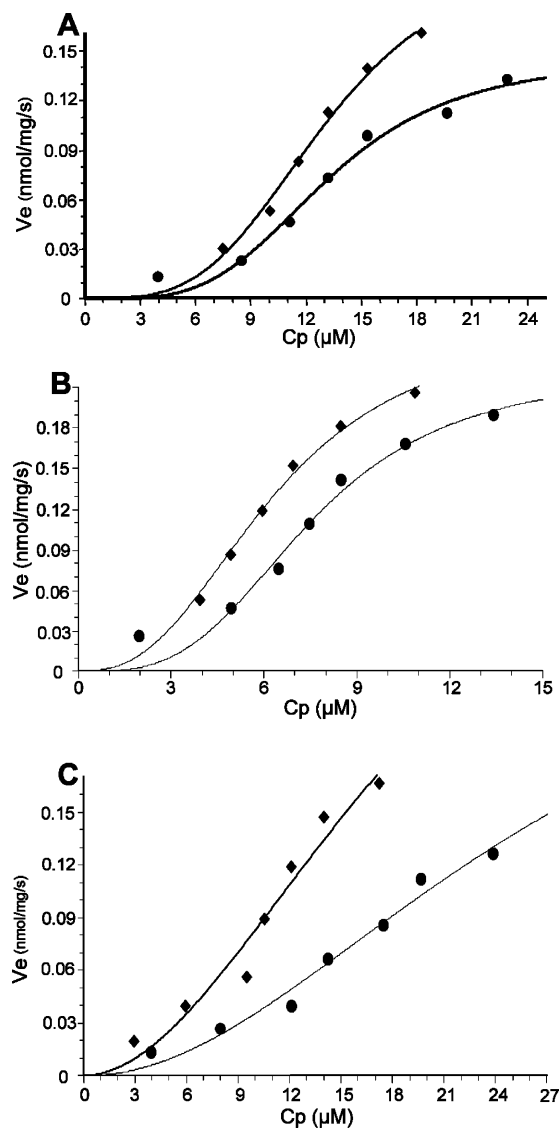


Figure 4. Stimulation of cefamandole efflux by 30 mM (A) and 0.1 mM (B) benzene, as well as 0.1 mM chloramphenicol (C). Measurement was carried out in the absence (■) and presence (◆) of stimulants. Each of these experiments was repeated several times, and reproducible results were obtained.

about 60%) in K_M . It was stimulated less strongly by the presence of 0.1 mM cyclohexane, however (Table 1).

Docking Studies. In an effort to understand the mechanism of stimulation of nitrocefin and cepharmandole efflux by various ligands, we examined the binding of the substrates and stimulants to the distal binding pocket of the binding protomer of AcrB with Autodock Vina. Initially, we focused on benzene and nitrocefin, which were predicted to bind to two distinct subareas of the binding pocket. Benzene was predicted to bind to the lower part of the pocket, previously named “cave”,⁶ with a low affinity (-5.1 kcal). Nitrocefin, which is predicted to bind very tightly to the pocket of the free AcrB (with the calculated energy of -10.2 kcal), was found to bind less tightly to AcrB with a prebound benzene (-9.4 kcal) as the thiophene ring of nitrocefin clashes with the benzene and was thus displaced by this molecule. As for cefamandole, it is predicted to bind somewhat less tightly (-9.2 kcal) than nitrocefin, exclusively to the upper, “groove” region

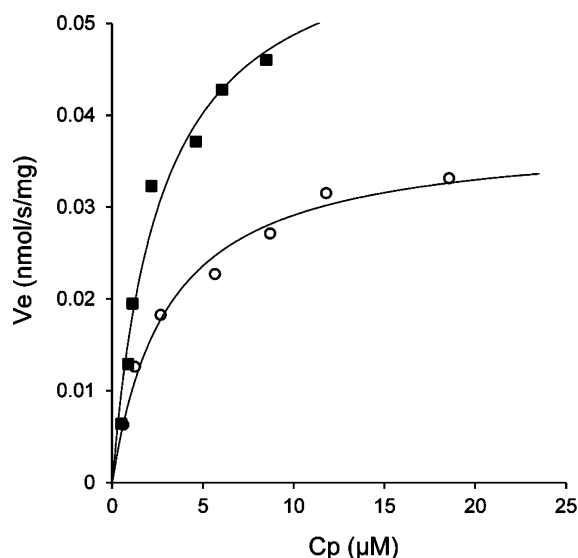


Figure 5. Stimulation of nitrocefin efflux occurs also in a covalently linked AcrB trimer. This figure shows a representative experiment in which nitrocefin efflux was measured in the absence (○) and presence (■) of 30 mM benzene.

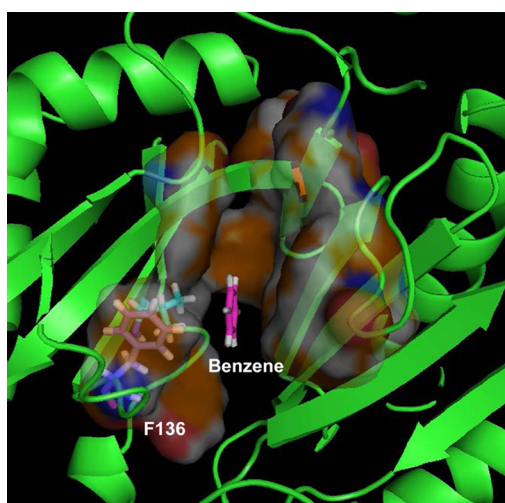


Figure 6. Docked position of benzene in the binding protomer of AcrB. F136 and V139 are shown in orange and green stick models. This image was produced by using the program PyMol.

of the pocket⁶ and thus will be less affected by the binding of benzene to the lower region of the pocket. However, Autodock Vina predicts that Arg β -naphthylamide binds tightly (-9.9 kcal) to the subdomain that is also occupied by nitrocefin, and the effort to dock nitrocefin to AcrB with the prebound Arg β -naphthylamide ended up with the prediction that nitrocefin will preferentially bind to sites that are completely outside of the pocket.

Similar docking studies were carried out with an MD-simulation-optimized model of V139F mutant AcrB. Compared with the wild type AcrB, benzene was indeed found to bind with a higher affinity (-8.5 kcal), and nitrocefin with a lower affinity (-8.6 kcal).

MD Simulation Studies. Because docking cannot take into account the effect of water molecules and the substrate-induced changes in the conformation of the binding site, we examined

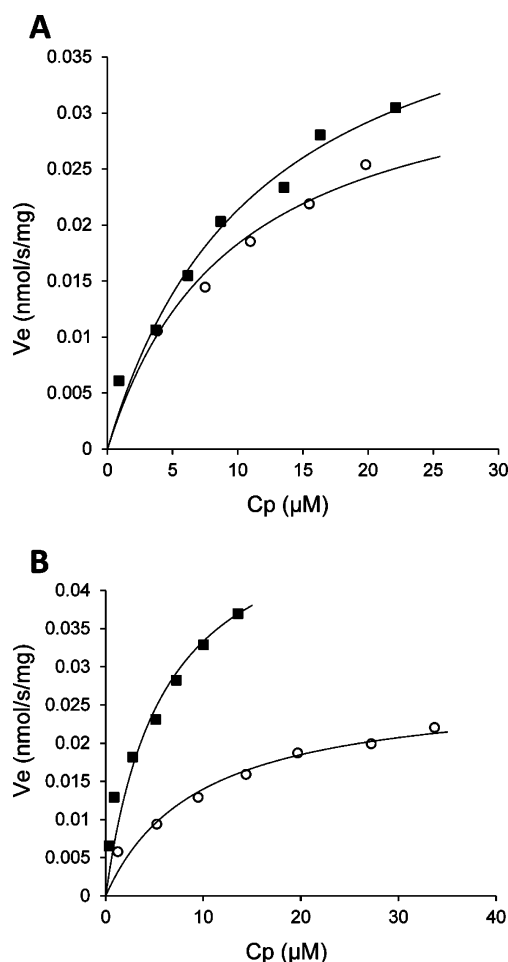


Figure 7. Stimulation of nitrocefin efflux by a low concentration (0.1 mM) of benzene. (A) Cells producing the wild type AcrB. (B) Cells producing the V139F mutant AcrB. These experiments were repeated several times, and similar results were obtained (see Table 1).

some of these interactions by MD simulations, concentrating on nitrocefin and benzene (Supplementary Table S1).

1. Benzene Alone. We started from the most stable docked structures of the benzene-(wild type)AcrB complex (Figure 8A). In one simulation, benzene kept hopping between two different positions in the binding site (Figure 8B,C and Supplementary Figures S2 and S3). Calculated binding free energies were similar at these two positions (Table 2). In another simulation, starting from a different but energy-equivalent binding pose, benzene remained essentially in the same, lower part of the binding pocket (Figures 8D). In all poses, benzene tended to be loosely surrounded by several hydrophobic residues, including the aromatic F136, F178, Y327, V571, F610, and F628 (Supplementary Table S2).

In the V139F AcrB, the initial docked position showed benzene indeed interacting more tightly (see above) with the phenyl group of the newly created F139 with a loose stacking interaction at the distance of about 4 Å (Figure 8E). At the end of MD simulations, the binding site has undergone significant changes of conformation, and in two independent MD simulations the benzene molecule became sandwiched between the F139 and F628 (Figure 8F,G), although its binding position did not change dramatically with respect to that in wild type AcrB (Supplementary Figure S3). Also the key residues stabilizing benzene within the pocket were well-conserved

Table 1. K_M and V_{max} of Nitrocefin Efflux

strains used	without additive		with additive		
	K_M	V_{max}	additive	K_M	V_{max}
wild type	10.3 ± 1.9 (9)	36.1 ± 9.8 (9)	0.1 mM benzene	6.4 ± 0.1 (3)	41 ± 12 (3)
			0.1 mM cyclohexane	7.0; 9.6	36; 26
			0.1 mM cyclohexanone	10.4 ± 2.6 (4)	47 ± 5 (4)
V139F	10.2 ± 2.8 (10)	43.7 ± 14.6 (10)	0.1 mM benzene	4.1 ± 1.8 (3)	46 ± 15 (3)
			0.1 mM cyclohexane	6.7 ± 2.6 (5)	48 ± 12 (5)
			0.1 mM cyclohexanone	5.1; 16.4	49; 72

K_M and V_{max} values shown are average ± SD, except in those cases where only two experiments were carried out, and in units of μM and pmol/s/mg (dry weight) cells, respectively. The numbers in parentheses show the number of independent experiments.

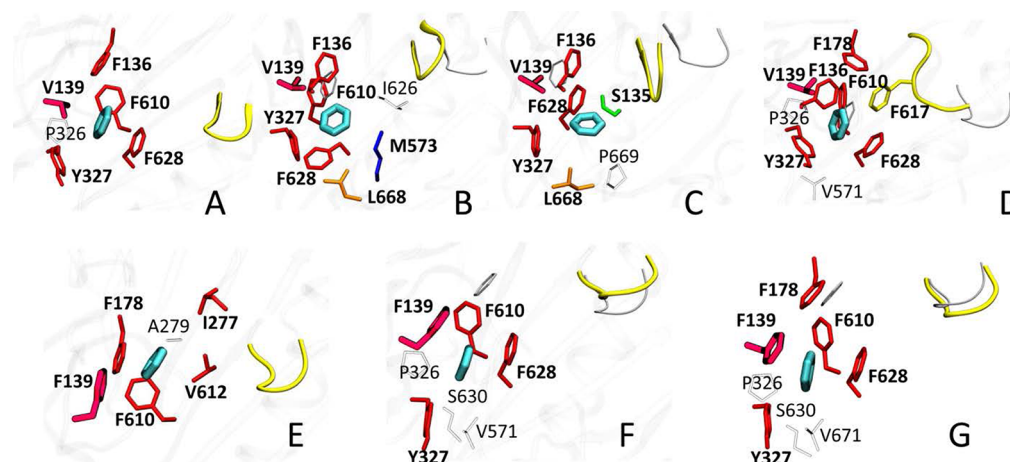


Figure 8. Binding of benzene to the distal pocket of wt (A–D) and V139F variant (E–G) of AcrB. Side chains of residues belonging to regions defined earlier⁹ and within 3.5 Å from benzene are shown with solid sticks, with the following color code: distal pocket, red; cleft, orange; proximal pocket, green; distal/proximal pocket interface, blue; G-loop, yellow. V/F139 are shown with thicker sticks. Benzene is shown with cyan sticks, and the G-loop is highlighted in yellow for each pose. Docking conformations of benzene and of the G-loop are shown in gray in B–D and F–G. Residues not belonging to any relevant region are shown with transparent sticks. (A) Docking position in wt AcrB. (B, C) Representative conformations, BNZ_{WT} (1₁) and BNZ_{WT} (1₂), sampled in simulation BNZ_{WT} (1). (D) Representative conformation from BNZ_{WT} (2). (E) Docking position of BNZ in V139F AcrB. (F, G) Representative conformations sampled in simulations BNZ_{V139F} (1) and BNZ_{V139F} (2).

compared to the complex with the unaltered AcrB (Supplementary Table S2).

In the MD simulations, benzene seemed to bind more stably to the V139F variant of AcrB (Supplementary Figure S3A), yet the MM/GBSA approach was unable to reflect this feature in the values of the binding free energy (see Table 2), possibly because the entropy term was not included.⁹ We therefore used a more powerful approach, metadynamics^{20–23} (see Experimental Procedure in Supporting Information) in order to evaluate the free energy cost associated with the displacement of benzene from the Phe-rich cage. This quantity can be related to the residence time of benzene in the binding pocket, which in turn might be inversely related to the rate at which AcrB conformational changes occur along the functional rotation cycles (see Discussion). We chose a simple and intuitive collective variable (CV) to be biased, i.e., the distance between the centers of mass of benzene and of residues surrounding it (see Supporting Information). The affinity of benzene was indeed higher for the mutated than for the wild type protein. Namely, the packing of the solvent by residues F136 and F139 increases by ~3 kcal/mol the free energy barrier associated to unbinding from the most stable position in the pocket (Supplementary Figure S4). In addition to the well-tempered metadynamics simulations, we performed an additional set of standard metadynamics simulations, without any wall on the distance between benzene and the center of mass of the pocket.

Interestingly, in three different simulations performed for each system, benzene exited the protein from the external cleft in the wild type complex and reached the exit gate in the mutated protein (data not shown). This surprising finding, however, is consistent with a larger stimulation, by benzene, of nitrocefin efflux in the V139F variant (Figure 7B).

2. Nitrocefin Alone. We extended to 165 ns the simulation of the nitrocefin-(wild type)AcrB reported earlier⁹ (Supplementary Table S1), but there were no significant changes in the binding position and affinity (Figure 9A,B and Table 2). When docking of nitrocefin was carried out with AcrB_{V139F}, the binding was weaker than with the wild type AcrB, as described above. One of the few prominent interaction was the loose (~4 Å) sandwiching of the thiophene ring of nitrocefin between F139 and F628 (Figure 9C). In the subsequent MD simulation nitrocefin contacts with the protein and water were optimized, and the thiophene ring lost contacts with F139 (Figure 9D).

3. Nitrocefin Binding to Benzene-AcrB Complex. We investigated how nitrocefin binding is affected by the presence of a benzene molecule in AcrB. When docking of nitrocefin was carried out using representative benzene-AcrB(wild type) conformations optimized by MD simulations, we found that it bound less tightly to the transporter: the binding energy calculated by Vina (obtained by empirical methods and cannot be compared to the free energies in Table 2) were in the range of –8.0 to –9.1 kcal/mol, weaker than the –10.2 kcal/mol

Table 2. Free Energies and Surface Matching Coefficients

Compound ^a	ΔG_b^b	% of ΔG_b						Surface Matching	
		Distal Pocket ^c	Proximal Pocket	G-loop	DP/PP Interface	External Cleft	BNZ/NCF	SM _{Tot} ^d	SM _L ^d
BNZ _{WT} (1 ₁)	-11.6 ± 1.3	-3.3 (28/59)			-0.4 (3/8)			1.00	1.00
BNZ _{WT} (1 ₂)	-11.0 ± 1.3	-1.8 (28/59)	-0.2 (1/3)	-0.2 (2/5)	-0.4 (3/9)	-0.7 (6/17)		0.96	0.98
BNZ _{WT} (2)	-11.9 ± 1.3	-3.3 (27/58)				-0.3 (2/6)		1.00	1.00
BNZ _{V139F} (1)	-12.3 ± 1.5	-3.4 (27/56)						1.00	1.00
BNZ _{V139F} (2)	-12.5 ± 1.2	-3.2 (24/55)						0.87	0.93
NCF _{WT}	-38.9 ± 3.8	-17.4 (44/68)	-1.2 (3/4)		-1.0 (2/3)			0.62	0.78
NCF _{V139F}	-42.0 ± 3.8	-14.1 (33/54)						0.49	0.63
NCF-BNZ _{WT} (1, NCF)	-34.2 ± 3.7	-11.2 (32/53)		-2.8 (8/13)			-0.6 (2)	nc ^e	nc
NCF-BNZ _{WT} (1, BNZ)	-12.2 ± 1.5	-2.6 (21/45)		-0.3 (2/5)	-0.3 (2/5)		-0.4 (3)	nc	nc
NCF-BNZ _{WT} (2, NCF)	-32.9 ± 4.4	-15.7 (47/65)						nc	nc
NCF-BNZ _{WT} (2, BNZ)	-13.0 ± 1.6	-2.3 (18/48)		-0.5 (3/9)	-0.4 (3/8)	-0.4 (3/8)		nc	nc
NCF-BNZ _{V139F} (1, NCF)	-41.2 ± 3.4	-18.2 (44/58)		-2.3 (5/7)				nc	nc
NCF-BNZ _{V139F} (1, BNZ)	-11.1 ± 1.8	-3.2 (28/60)			-0.5 (4/9)			nc	nc
NCF-BNZ _{V139F} (2, NCF)	-41.1 ± 2.8	-18.0 (42/64)						nc	nc
NCF-BNZ _{V139F} (2, BNZ)	-12.4 ± 1.2	-3.3 (26/56)			-0.2 (1/3)			nc	nc

^aThe contribution of the configurational entropy of the solute has not been included (see Supporting Information). Concerning the contributions of different regions to ΔG_b , only those larger than 2% are listed. ^bNumbers 1 and 2 in parentheses refer to the simulation number thereon, with BNZ_{WT} (1₁) and BNZ_{WT} (1₂) indicating the two clusters of conformations found in the simulation of BNZ_{WT} (1). The calculations for all compounds refer to the drugs bound to the distal pocket of the binding protomer. BNZ and NCF refer to benzene and nitrocefin, respectively. ^cResidues within the various regions are listed in Figure 1 of ref 9. The numbers in parentheses before and after the slash indicate respectively the percentage with respect to the binding free energy and to the sum of the contributions from all residues. ^dCalculated on the conformation of the complex with the lower RMSD from the average extracted from the unbiased MD simulations. SM_{Tot} and SM_L refer to the total and lipophilic surface matching coefficients. See Supporting Information for further details. ^enc: not calculated.

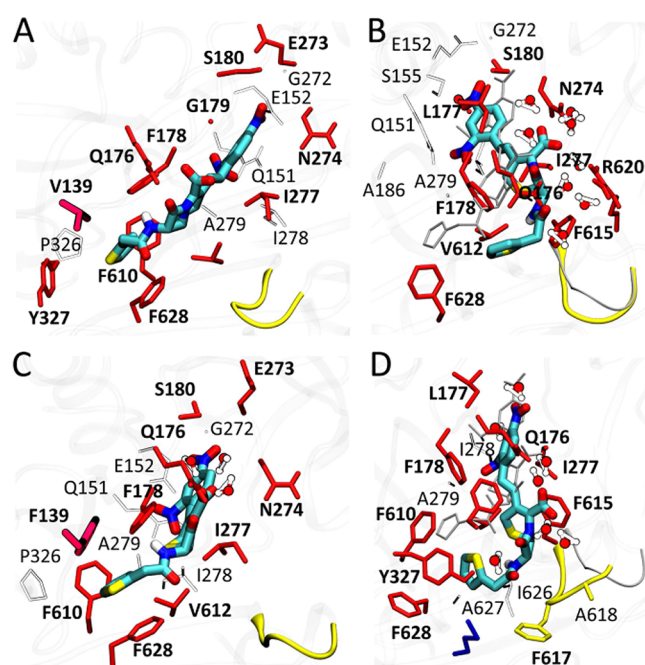


Figure 9. Binding of nitrocefin to the distal pocket of wt (A, B) and V139F variant (C, D) of AcrB. (A) Docking position in wt AcrB. (B) Representative conformations sampled in NCF_{WT}. (C) Docking position in the V139F AcrB. (D) Representative conformations sampled in NCF_{V139F} (1).

energy obtained for wild type AcrB free of benzene. Two opposite orientations of nitrocefin were found to be compatible with prebound benzene in the distal pocket (data not shown). The difference in affinity compared to the bimolecular complex was retained in the binding free energy calculated over the two

MD trajectories (one per orientation of nitrocefin) of the trimolecular system nitrocefin-benzene-AcrB (Table 2).

Interestingly, compared with the bimolecular complexes, in one of the MD simulations benzene moved by a few Å toward the upper part of the distal pocket (Figure 10A), and the pattern of stabilizing contacts was only partly conserved (Supplementary Table S2). In both wild type and mutant trimolecular complexes, nitrocefin moved more significantly in the direction of the Exit Gate toward the TolC docking domain,¹¹ with the carboxyl group facing residues Q124 and Y758 (compare the stick models of nitrocefin in green and lime with those in red and mauve in Figure 10B). This movement of the substrate was also seen in the second MD simulation started from a different conformation of the benzene-AcrB complex (where nitrocefin assumed a flipped orientation with respect to the first simulation, see Supplementary Figures S5A and S5C), although its magnitude was somewhat less (Supplementary Table S1). In this case the axis of nitrocefin was not fully aligned to the Binding Pocket-Gate direction. Several key interactions with residues of the binding pocket were retained despite this displacement (Supplementary Table S3), although the overall interaction strength was reduced (Table 2). MD simulations thus showed that the two substrates can bind simultaneously to the distal pocket, benzene in the bottom and nitrocefin (in two opposite orientations) in the upper part, closer to the Exit Gate.

DISCUSSION

We detected some hints earlier⁶ that the presence of one ligand, chloramphenicol, may enhance the efflux of another ligand, nitrocefin, added at the same time. The differences were small, yet this conclusion could be confirmed in the present study (Figure 1). We further showed in this study that, when tested at high concentrations (around 30 mM), simple solvents such as

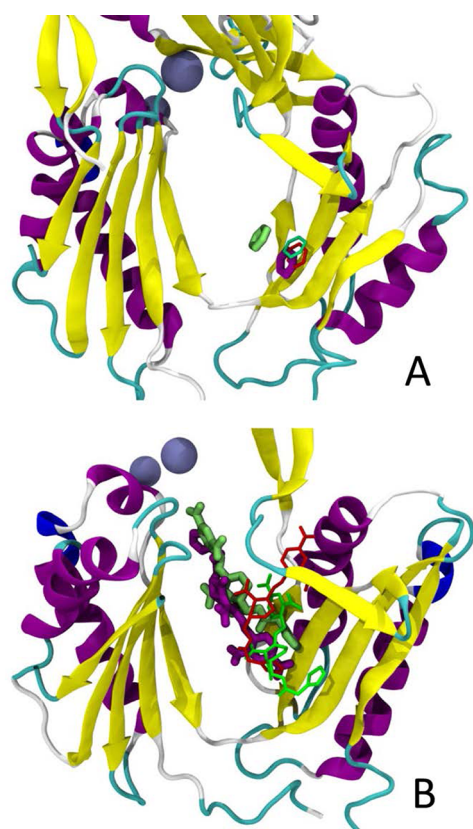


Figure 10. Binding positions of benzene (A) and nitrocefin (B) in the bi- and trimolecular complexes with AcrB. Thinner and thicker sticks represents the ligands in the bimolecular and trimolecular adducts, respectively. Red and magenta indicate the wt complexes, while green and lime indicate the mutated ones. The protein is shown in cartoons and is colored according to the secondary structure. Residues Q124 and Y758 lining the gate to the central funnel are shown with ice blue beads.

benzene, cyclohexane, and cyclohexanone stimulated much more strongly the efflux of nitrocefin, partly by increasing its V_{\max} for transport (Figure 2). Other than the solvents, Arg β -naphthylamide stimulated nitrocefin efflux strongly (Figure 3). In a mutant AcrB (V139F), benzene could produce a strong stimulation of nitrocefin efflux even at a low concentration of 0.1 mM (Figure 7B). Finally, benzene and chloramphenicol produced a modest but reproducible stimulation of the efflux of cefamandole (Figure 4), another cephalosporin.

Stimulation, by one substrate, of the efflux of another substrate is not unknown in the behavior of multidrug transporters. It is well-known that the transport of Hoechst 33342 dye by the P-glycoprotein is stimulated by the simultaneous presence of another substrate, rhodamine 123,^{25,24} an observation that led to the assumption that there are two distinct substrate binding sites (H-site and R-site for the Hoechst dye and rhodamine, respectively) that are separated by a measurable distance.²⁶ Similar stimulation phenomena were also found in the relatives of P-glycoprotein, multidrug resistance-associated proteins or MRPs.²⁷ Since P-glycoprotein functions as a monomer, such stimulation phenomena likely involve allosteric conformational changes introduced by the binding of one of the substrates.²⁸ In contrast, AcrB operates as a trimer, and the binding and export of substrates presumably involves tight interaction between the

neighboring protomers;^{11,29,30} thus the mechanism of stimulation may be more complex.

One trivial mechanism involves the accelerated assembly of AcrB trimer by the stimulator substrate, but we were able to show that this mechanism cannot explain our observations, because even covalently linked trimeric AcrB was stimulated by benzene (Figure 5). (However, at present we cannot rule out the possibility that the assembly of the AcrB-AcrA-TolC tripartite complex might be affected.) In the next step, we considered the interaction between the substrates within a single AcrB protomer, by examining the binding of substrates to the distal binding pocket of AcrB, which plays a critical role in the export process.^{30,31} Computational docking suggested that the initial binding of benzene to the “lower” part of this pocket weakens the subsequent binding of nitrocefin, mainly to the “upper” part of the pocket, a conclusion supported by the MD simulation, showing 5–6 kcal/mol decrease in the absolute value of the binding energy of nitrocefin when benzene was simultaneously present in the pocket (Table 2). Since nitrocefin appears to bind to the pocket of AcrB exceptionally tightly, as judged by its very low transport K_M value⁷ and its large calculated binding energy (see Table 2 of our previous paper⁷), it seemed possible, a priori, that a weakened binding of this substrate may explain its increased efflux by the minimization of the energy trough of binding. However, there are several lines of evidence against this hypothesis. First, the efflux of cefamandole, which appears to bind to the pocket much more loosely than nitrocefin on the basis of its higher transport K_M (actually $K_{0.5}$)⁷ and the smaller binding energy than nitrocefin (see Results), is nevertheless stimulated by the presence of benzene (Figure 4). Second, in the strain expressing the V139F mutant AcrB, benzene causes hardly a decrease in the binding energy of nitrocefin (Table 2), although benzene strongly stimulates nitrocefin efflux (Figure 7). Third, it is difficult to explain, by this hypothesis, the strong stimulation of nitrocefin efflux caused by Arg β -naphthylamide, because both substrates are expected to bind to a similar area of the pocket.

In fact, MD simulations gave us some hints that may at least partially explain the efflux stimulation data. When nitrocefin was present together with benzene in the binding site, the former was eventually pushed for about 7 Å toward the exit gate (Figure 10B), suggesting that the presence of benzene could favor the accelerated efflux of nitrocefin. In addition, more than one molecule of small substrates, such as benzene, may bind to the same binding pocket at the same time, and this could produce stimulation of efflux.

An important factor we have not considered may be the binding of substrates in successive binding pockets in the same AcrB protomer or in different protomers within the trimeric assembly. Thus the existence of a more proximal binding pockets, earlier identified in the symmetric AcrB crystals^{32–35} and by Cys mutagenesis studies,³¹ was now confirmed to be present in the Access protomer by crystallography involving asymmetric crystals.^{36,37} The extrusion of a drug molecule bound in the binding protomer thus would either require, or be at least stimulated by, the binding of the next drug molecule to the proximal binding site of the neighboring Access protomer. It seems likely that the “stimulating” substrate, such as solvents or Arg β -naphthylamide, could affect the efflux of the measured substrate, such as nitrocefin or cefamandole bound in the Binding protomer, in this manner. The stimulation by Arg β -naphthylamide, a large compound that is predicted to bind to

the same area in the distal binding pocket as nitrocefin, seems to require such a mechanism. Such interaction between the neighboring protomers was indeed the mechanism proposed to explain the positive cooperativity in the efflux of various cephalosporins⁷ and penicillins.³⁸ If this is the case, the efflux of cefamandole is limited by the rate at which the neighboring Access protomer would bind the next cefamandole molecule when it is the only substrate present. Since solvent molecules are predicted to enter (and exit) the AcrB binding pockets rapidly, as discussed below, the cefamandole efflux is likely accelerated by the rapid entry of solvents (and other substrates that are pumped out rapidly) into the neighboring Access protomer, when these substrates are also present. We indeed found that benzene decreased the Hill coefficient for the efflux of cefamandole, an observation that supports our hypothesis. Cefamandole and solvent molecules could also bind to the same protomer and could be extruded simultaneously.

It is well-known that AcrB pumps out solvents.⁵ Importantly this efflux seems to occur with very high turnover numbers. Although the kinetic constants of benzene efflux through AcrB are not known, we can make a rough estimate as follows. The permeability coefficient of benzene in a conventional phospholipid bilayer was estimated as 9.9 cm/s by MD simulations.³⁹ Assuming that the outer membrane bilayer has permeability about 3 orders of magnitude lower than that of the conventional bilayer,⁴⁰ we can estimate the permeability coefficient of benzene here as 0.01 cm/s. Thus if AcrB decreases the periplasmic benzene concentration by 10% when the cells are exposed to 100 μ M benzene, creating a 10 μ M concentration gradient across the outer membrane, benzene will diffuse into the periplasm at a rate of 13.2 nmol/mg cells/s. To counteract this influx, AcrB must pump out the solvent at about this rate. This can be compared with the low V_{\max} values for the efflux of nitrocefin and cefamandole (0.02 and 0.4 nmol/mg cells/s, respectively).⁷ Similarly, although the efflux rate of chloramphenicol is not known, we can assume that it is rapid, as it must penetrate across the outer membrane, mainly through the porin channels, rapidly as it is relatively small and uncharged.⁴¹ These considerations suggest that the stimulators of cephalosporin efflux in AcrB are likely to be compounds that are very rapidly pumped out as substrates.

In general, it is difficult to know the rate-limiting steps in a secondary transporter. However, in one case that has been studied extensively, LacY of *E. coli*, it appears to be the rate of conformational alteration generating the outward-open conformer, rather than the rate of substrate binding.⁴² Perhaps in AcrB also, it seems possible that various substrates facilitate, to a different degree, the large conformational change from the Binding to Extrusion conformation^{11,29,30} necessary for the drug export. Finally it is also possible that stimulator substrates enter rapidly into the deep binding pocket without being trapped in the proximal binding pocket,⁴³ thereby producing an accelerated functional cycle through which the efflux of other larger substrates becomes accelerated.

■ ASSOCIATED CONTENT

● Supporting Information

Details of experimental procedures and additional figures. This material is available free of charge via the Internet at <http://pubs.acs.org>.

■ AUTHOR INFORMATION

Corresponding Author

*Phone: 510-642-2027. E-mail: nhirosi@berkeley.edu.

Funding

This study was supported in part by a grant from U.S. Public Health Service AI-009644 (to H.N.).

Notes

The authors declare no competing financial interest.

■ ACKNOWLEDGMENTS

A.V.V. thanks Paolo Ruggerone for useful discussions and continuous support. The authors acknowledge gratefully computational resources from the Lawrence Berkeley National Laboratory (Berkeley, CA) and from CINECA (Bologna, Italy; PRACE fourth Call grant "Understanding the bacterial efflux systems: insights into structure–function relationship from all-atom simulations" and ISCRA-A Grant HP10ARSZ26).

■ ABBREVIATIONS

PCR, polymerase chain reaction; MD, molecular dynamics

■ REFERENCES

- (1) Saier, M. H., Jr., Paulsen, I. T., Sliwinski, M. K., Pao, S. S., Skurray, R. A., and Nikaido, H. (1998) Evolutionary origins of multidrug and drug-specific efflux pumps in bacteria. *FASEB J.* 12, 265–274.
- (2) Nikaido, H. (1996) Multidrug efflux pumps of gram-negative bacteria. *J. Bacteriol.* 178, 5853–5859.
- (3) Ma, D., Alberti, M., Lynch, C., Nikaido, H., and Hearst, J. E. (1996) The local repressor AcrR plays a modulating role in the regulation of *acrAB* genes of *Escherichia coli* by global stress signals. *Mol. Microbiol.* 19, 101–112.
- (4) Tsukagoshi, N., and Aono, R. (2000) Entry into and release of solvents by *Escherichia coli* in an organic-aqueous two-liquid-phase system and substrate specificity of the AcrAB-TolC solvent-extruding pump. *J. Bacteriol.* 182, 4803–4810.
- (5) White, D. G., Goldman, J. D., Demple, B., and Levy, S. B. (1997) Role of the *acrAB* locus in organic solvent tolerance mediated by expression of *marA*, *soxS*, or *robA* in *Escherichia coli*. *J. Bacteriol.* 179, 6122–6126.
- (6) Takatsuka, Y., Chen, C., and Nikaido, H. (2010) Mechanism of recognition of compounds of diverse structures by the multidrug efflux pump AcrB of *Escherichia coli*. *Proc. Natl. Acad. Sci. U.S.A.* 107, 6559–6565.
- (7) Nagano, K., and Nikaido, H. (2009) Kinetic behavior of the major multidrug efflux pump AcrB of *Escherichia coli*. *Proc. Natl. Acad. Sci. U.S.A.* 106, 5854–5858.
- (8) Link, A. J., Phillips, D., and Church, G. M. (1997) Methods for generating precise deletions and insertions in the genome of wild-type *Escherichia coli*: application to open reading frame characterization. *J. Bacteriol.* 179, 6228–6237.
- (9) Vargiu, A. V., and Nikaido, H. (2012) Multidrug binding properties of the AcrB efflux pump characterized by molecular dynamics simulations. *Proc. Natl. Acad. Sci. U.S.A.* 109, 20637–20642.
- (10) Trott, O., and Olson, A. J. (2010) AutoDock Vina: improving the speed and accuracy of docking with a new scoring function, efficient optimization, and multithreading. *J. Comput. Chem.* 31, 455–461.
- (11) Sennhauser, G., Amstutz, P., Briand, C., Storchenegger, O., and Grutter, M. G. (2007) Drug export pathway of multidrug exporter AcrB revealed by DARPIn inhibitors. *PLoS Biol.* 5, e7.
- (12) Humphrey, W., Dalke, A., and Schulten, K. (1996) VMD: Visual molecular dynamics. *J. Mol. Graphics Modell.* 14, 33–38.
- (13) Vargiu, A. V., Collu, F., Schulz, R., Pos, K. M., Zacharias, M., Kleinekathofer, U., and Ruggerone, P. (2011) Effect of the F610A mutation on substrate extrusion in the AcrB transporter: explanation

and rationale by molecular dynamics simulations. *J. Am. Chem. Soc.* 133, 10704–10707.

(14) Elkins, C. A., and Nikaido, H. (2002) Substrate specificity of the RND-type multidrug efflux pumps AcrB and AcrD of *Escherichia coli* is determined predominantly by two large periplasmic loops. *J. Bacteriol.* 184, 6490–6498.

(15) Lomovskaya, O., Warren, M. S., Lee, A., Galazzo, J., Fronko, R., Lee, M., Blais, J., Cho, D., Chamberland, S., Renau, T., Leger, R., Hecker, S., Watkins, W., Hoshino, K., Ishida, H., and Lee, V. J. (2001) Identification and characterization of inhibitors of multidrug resistance efflux pumps in *Pseudomonas aeruginosa*: novel agents for combination therapy. *Antimicrob. Agents Chemother.* 45, 105–116.

(16) Lamers, R. P., Cavallari, J. F., and Burrows, L. L. (2013) The efflux inhibitor phenylalanine-arginine beta-naphthylamide (PAβN) permeabilizes the outer membrane of gram-negative bacteria. *PLoS One* 8, e60666.

(17) Matsumoto, Y., Hayama, K., Sakakihara, S., Nishino, K., Noji, H., Iino, R., and Yamaguchi, A. (2011) Evaluation of multidrug efflux pump inhibitors by a new method using microfluidic channels. *PLoS One* 6, e18547.

(18) Lomovskaya, O., and Bostian, K. A. (2006) Practical applications and feasibility of efflux pump inhibitors in the clinic—a vision for applied use. *Biochem. Pharmacol.* 71, 910–918.

(19) Takatsuka, Y., and Nikaido, H. (2009) Covalently linked trimer of the AcrB multidrug efflux pump provides support for the functional rotating mechanism. *J. Bacteriol.* 191, 1729–1737.

(20) Barducci, A., Bussi, G., and Parrinello, M. (2008) Well-tempered metadynamics: A smoothly converging and tunable free-energy method. *Phys. Rev. Lett.* 100, 020603.

(21) Biarnes, X., Bongarzone, S., Vargiu, A. V., Carloni, P., and Ruggerone, P. (2011) Molecular motions in drug design: the coming age of the metadynamics method. *J. Comput.-Aided Mol. Des.* 25, 395–402.

(22) Laio, A., and Parrinello, M. (2002) Escaping free-energy minima. *Proc. Natl. Acad. Sci. U.S.A.* 99, 12562–12566.

(23) Vargiu, A. V., Ruggerone, P., Magistrato, A., and Carloni, P. (2008) Dissociation of minor groove binders from DNA: insights from metadynamics simulations. *Nucleic Acids Res.* 36, 5910–5921.

(24) Shapiro, A. B., and Ling, V. (1997) Positively cooperative sites for drug transport by P-glycoprotein with distinct drug specificities. *Eur. J. Biochem.* 250, 130–137.

(25) Shapiro, A. B., Fox, K., Lam, P., and Ling, V. (1999) Stimulation of P-glycoprotein-mediated drug transport by prazosin and progesterone. Evidence for a third drug-binding site. *Eur. J. Biochem.* 259, 841–850.

(26) Lugo, M. R., and Sharom, F. J. (2005) Interaction of LDS-751 with P-glycoprotein and mapping of the location of the R drug binding site. *Biochemistry* 44, 643–655.

(27) Borst, P., Zelcer, N., van de Wetering, K., and Poolman, B. (2006) On the putative co-transport of drugs by multidrug resistance proteins. *FEBS Lett.* 580, 1085–1093.

(28) Martin, C., Berridge, G., Higgins, C. F., Mistry, P., Charlton, P., and Callaghan, R. (2000) Communication between multiple drug binding sites on P-glycoprotein. *Mol. Pharmacol.* 58, 624–632.

(29) Murakami, S., Nakashima, R., Yamashita, E., Matsumoto, T., and Yamaguchi, A. (2006) Crystal structures of a multidrug transporter reveal a functionally rotating mechanism. *Nature* 443, 173–179.

(30) Seeger, M. A., Schiefner, A., Eicher, T., Verrey, F., Diederichs, K., and Pos, K. M. (2006) Structural asymmetry of AcrB trimer suggests a peristaltic pump mechanism. *Science* 313, 1295–1298.

(31) Husain, F., and Nikaido, H. (2010) Substrate path in the AcrB multidrug efflux pump of *Escherichia coli*. *Mol. Microbiol.* 78, 320–330.

(32) Yu, E. W., Aires, J. R., McDermott, G., and Nikaido, H. (2005) A periplasmic drug-binding site of the AcrB multidrug efflux pump: a crystallographic and site-directed mutagenesis study. *J. Bacteriol.* 187, 6804–6815.

(33) Drew, D., Klepsch, M. M., Newstead, S., Flaig, R., De Gier, J. W., Iwata, S., and Beis, K. (2008) The structure of the efflux pump AcrB in complex with bile acid. *Mol. Membr. Biol.* 25, 677–682.

(34) Hung, L. W., Kim, H. B., Murakami, S., Gupta, G., Kim, C. Y., and Terwilliger, T. C. (2013) Crystal structure of AcrB complexed with linezolid at 3.5 Å resolution. *J. Struct. Funct. Genomics* 14, 71–75.

(35) Tornroth-Horsefield, S., Gourdon, P., Horsefield, R., Brive, L., Yamamoto, N., Mori, H., Snijder, A., and Neutze, R. (2007) Crystal structure of AcrB in complex with a single transmembrane subunit reveals another twist. *Structure* 15, 1663–1673.

(36) Eicher, T., Cha, H. J., Seeger, M. A., Brandstatter, L., El-Delik, J., Bohnert, J. A., Kern, W. V., Verrey, F., Grutter, M. G., Diederichs, K., and Pos, K. M. (2012) Transport of drugs by the multidrug transporter AcrB involves an access and a deep binding pocket that are separated by a switch-loop. *Proc. Natl. Acad. Sci. U.S.A.* 109, 5687–5692.

(37) Nakashima, R., Sakurai, K., Yamasaki, S., Nishino, K., and Yamaguchi, A. (2011) Structures of the multidrug exporter AcrB reveal a proximal multisite drug-binding pocket. *Nature* 480, 565–569.

(38) Lim, S. P., and Nikaido, H. (2010) Kinetic parameters of efflux of penicillins by the multidrug efflux transporter AcrAB-TolC of *Escherichia coli*. *Antimicrob. Agents Chemother.* 54, 1800–1806.

(39) Bemporad, D., Luttmann, C., and Essex, J. W. (2005) Behaviour of small solutes and large drugs in a lipid bilayer from computer simulations. *Biochim. Biophys. Acta* 1718, 1–21.

(40) Plésiat, P., and Nikaido, H. (1992) Outer membranes of gram-negative bacteria are permeable to steroid probes. *Mol. Microbiol.* 6, 1323–1333.

(41) Nikaido, H., and Rosenberg, E. Y. (1983) Porin channels in *Escherichia coli*: studies with liposomes reconstituted from purified proteins. *J. Bacteriol.* 153, 241–252.

(42) Smirnova, I., Kasho, V., and Kaback, H. R. (2011) Lactose permease and the alternating access mechanism. *Biochemistry* 50, 9684–9693.

(43) Ruggerone, P., Murakami, S., Pos, K. M., and Vargiu, A. V. (2013) RND efflux pumps: structural information translated into function and inhibition mechanisms. *Curr. Top. Med. Chem.*, in press.